

General Solution for Diffusion-Controlled Dissolution of Spherical Particles. 1. Theory

JIANZHUO WANG AND DOUGLAS R. FLANAGAN*

Contribution from *Division of Pharmaceutics, College of Pharmacy, The University of Iowa, Iowa City, Iowa 52242.*

Received June 2, 1998. Final revised manuscript received January 20, 1999.
Accepted for publication March 9, 1999.

Abstract □ Three classical particle dissolution rate expressions are commonly used to interpret particle dissolution rate phenomena. Our analysis shows that an assumption used in the derivation of the traditional cube-root law may not be accurate under all conditions for diffusion-controlled particle dissolution. Mathematical analysis shows that the three classical particle dissolution rate expressions are approximate solutions to a general diffusion layer model. The cube-root law is most appropriate when particle size is much larger than the diffusion layer thickness, the two-thirds-root expression applies when the particle size is much smaller than the diffusion layer thickness. The square-root expression is intermediate between these two models. A general solution to the diffusion layer model for monodispersed spherical particles dissolution was derived for sink and nonsink conditions. Constant diffusion layer thickness was assumed in the derivation. Simulated dissolution data showed that the ratio between particle size and diffusion layer thickness (a_0/h) is an important factor in controlling the shape of particle dissolution profiles. A new semiempirical general particle dissolution equation is also discussed which encompasses the three classical particle dissolution expressions. The success of the general equation in explaining limitations of traditional particle dissolution expressions demonstrates the usefulness of the general diffusion layer model.

Dissolution phenomena have been studied in a quantitative manner for more than a century. The dissolution of solid particles is more complicated than that of constant surface area tablets because of surface area and/or shape changes during dissolution. Though particle dissolution models have been developed, discrepancies between theory and experimental data are present. It has not been shown whether these discrepancies are due to experimental factors or limitations of the mathematical models.

Two steps are involved in solid particle dissolution: the first step is the detachment of molecules from the solid surface to form hydrated molecules at the solid-liquid interface; the second step is the mass transport from this interface to the bulk solution. Most dissolution processes are controlled by the second step which is diffusion-convection-controlled. The basic diffusion-controlled model for solid dissolution was developed by Noyes and Whitney¹ and later modified by Nernst² and Brunner.³ This model assumes that rapid equilibrium (i.e., saturation) is achieved at the solid-liquid interface and then diffusion occurs across a thin layer of solution, called the diffusion layer, into the bulk solution. Diffusion across this diffusion layer is rate-controlling in most cases, which effectively converts the heterogeneous process of dissolution to a homogeneous process of liquid-phase diffusion. Nernst and Brunner's concept of a diffusion layer being a stagnant or unstirred layer of liquid adhering to the solid surface is naive but allows complex dissolution processes to be analyzed in a

tractable fashion. However, as pointed out by King,⁴ this layer need not be stagnant and can be a hydrodynamic boundary which has a velocity as well as a concentration gradient.

Three diffusion-controlled models have been reported for single spherical particle dissolution under sink conditions, as shown below:

$$w^{1/3} = w_0^{1/3} - k_{1/3}t \quad k_{1/3} = \left(\frac{4\pi\rho}{3}\right)^{1/3} \frac{DC_S}{\rho h} \quad (\text{eq 1})$$

$$w^{1/2} = w_0^{1/2} - k_{1/2}t \quad k_{1/2} = \left(\frac{3\pi\rho}{2}\right)^{1/2} \frac{DC_S}{K\rho} \quad (\text{eq 2})$$

$$w^{2/3} = w_0^{2/3} - k_{2/3}t \quad k_{2/3} = \left(\frac{4\pi\rho}{3}\right)^{2/3} \frac{2DC_S}{\rho} \quad (\text{eq 3})$$

where w is particle weight at time t , w_0 is initial particle weight, $k_{1/3}$, $k_{1/2}$, and $k_{2/3}$ are composite rate constants, ρ is the density of the particle, D is diffusion coefficient, C_S is solubility, h is diffusion layer thickness, and K is a constant. Equation 1 was derived by Hixson and Crowell⁵ and is known as the "cube-root law". Equation 2 is the semiempirical expression reported by Niebergall et al.⁶ and has a square-root dependency on weight. Equation 3 was derived by Higuchi and Hiestand⁷ and has a two-thirds-root dependency on weight. Each of the above equations gives satisfactory fits to certain experimental dissolution data.^{6,8,9} These three expressions are still the basis for particle dissolution theories in contemporary dissolution testing.¹⁰ However, the choice of the model to fit experimental data is still somewhat arbitrary. Though they appear different in form, the three equations are difficult to distinguish when applied to experimental data. A particular dissolution profile can often be fitted by at least two of these equations almost equally well.¹¹ Thus, it seems that dissolution behavior of simple spherical particles is still not theoretically well defined.

Among the three equations, the most commonly used is the "cube-root law". The cube-root law was first derived by assuming that dissolution rate is proportional to particle surface area. Though Hixson and Crowell did not specifically use the diffusion layer model to derive their equation, the cube-root law can also be derived from a simple diffusion layer model. Our further analysis shows that the cube-root law is only an approximate solution to the diffusion layer model, because an assumption used may not be accurate under all conditions for diffusion-controlled particle dissolution.

Below are dissolution rate expressions for the diffusion layer model:

$$\frac{dQ}{dt} = \frac{DA}{h} (C_S - C_b) \quad (\text{eq 4})$$

$$\frac{dQ}{dt} = -DA \left. \frac{\partial C}{\partial r} \right|_{r=a} \quad (\text{eq 5})$$

* Corresponding author. Ph: 319-335-8827. Fax: 319-335-9349.
E-mail: douglas-flanagan@uiowa.edu.

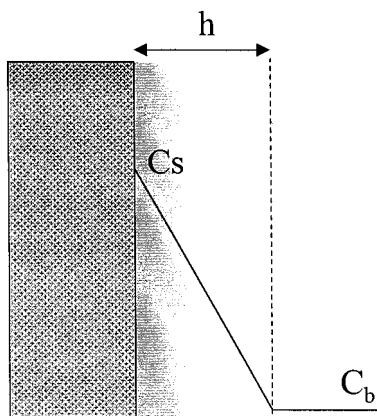


Figure 1—Steady-state concentration gradient around a planar surface.

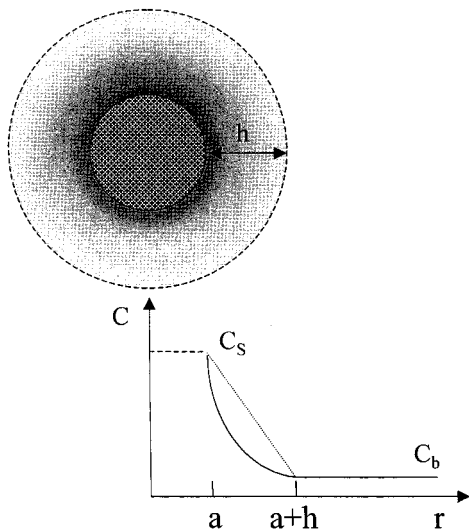


Figure 2—Pseudo-steady-state concentration gradient around a spherical particle (radius = a).

where dQ/dt is the rate of dissolution, A is particle surface area, h is the thickness of the diffusion layer, C_b is bulk solution concentration, r is the distance from the center of the particle, and a is particle radius. Equation 4 is exact for planar surface dissolution under sink conditions, because the concentration gradient in the diffusion layer is linear at steady-state (Figure 1). However, for a curved surface, eq 4 is not accurate because the concentration gradient around a spherical particle is not linear under pseudo-steady-state conditions (Figure 2). Particle dissolution rate expressions based on eq 4 will not give accurate solutions to the diffusion layer model for spherical particles. For more accurate results, the derivation should start from eq 5 which is Fick's first law expression for spherical geometry.

For particle dissolution, changing bulk solution concentration complicates the mathematical analysis. Most researchers use sink conditions to make the treatment of experimental data easier. The three traditional particle dissolution expressions are such examples, which is what we emphasize here. A general (and more exact) solution to the diffusion layer model for spherical particle dissolution under sink conditions will be derived, and the relationship between the general solution and the classical expressions will be discussed. A general solution for spherical particle dissolution under nonsink conditions is also included and briefly discussed. Understanding the limitations of the three classical particle dissolution expressions will make it easier to use them appropriately. The availability of the general solution will provide a sound basis for

determining whether diffusion layer thickness is dependent upon particle size, which has been a point of discussion.^{6,10,12-14} It also provides a sound basis for the investigation of polydispersity effects on particle dissolution.

Theory

The diffusion layer model for single spherical particle dissolution under sink conditions is based on the following assumptions:

- The particle is spherical and dissolves isotropically.
- The particle is in a well-stirred solution and there exists a boundary layer around the particle of constant thickness (h).
- During dissolution, a pseudo-steady-state is established with only minimal solid dissolution, after which the overall mass transport rates across the inner and outer spherical surfaces (at $r = a$ and $a + h$) of the diffusion layer are assumed to be equal.¹⁵
- The concentration at the interface between the solid and the solution is saturated (C_s), and solubility is independent of particle size.
- The bulk solution concentration (C_b) is assumed to be zero, and the diffusion coefficient (D) is a constant throughout the diffusion layer.

Since the concentration gradient around a spherical particle is not linear at pseudo-steady-state, it is a function of distance from the center of the particle. The function $G(R)$ can be defined as the concentration gradient at a distance R from the center of the particle and is given by:

$$G(R) \equiv \left. \frac{\partial C}{\partial r} \right|_{r=R}$$

With this definition, eq 5 becomes:

$$\frac{dQ}{dt} = -DAG(a) \quad (\text{eq 6})$$

The surface area of a sphere is $4\pi r^2$ and applying the pseudo-steady-state assumption c gives:

$$4\pi a^2 G(a) = 4\pi r^2 G(r) \quad a \leq r \leq a + h \quad (\text{eq 7})$$

and

$$G(r) = \frac{a^2}{r^2} G(a) \quad (\text{eq 8})$$

Using assumptions d and e, the total concentration difference across the diffusion layer is C_s , which leads to:

$$\int_a^{a+h} -G(r) dr = C_s \quad (\text{eq 9})$$

Substituting eq 8 into eq 9 gives:

$$\int_a^{a+h} -\frac{a^2}{r^2} G(a) dr = C_s \quad (\text{eq 10})$$

Integrating eq 10 gives:

$$G(a) = -C_s \left(\frac{1}{a} + \frac{1}{h} \right) \quad (\text{eq 11})$$

Substituting eq 11 into eq 6 gives:

$$\frac{dQ}{dt} = DAC_s \left(\frac{1}{a} + \frac{1}{h} \right) \quad (\text{eq 12})$$

Using $4\pi a^2$ for area (A) in eq 12 gives:

$$\frac{dQ}{dt} = 4\pi a^2 DC_S \left(\frac{1}{a} + \frac{1}{h} \right) \quad (\text{eq 13})$$

Considering the change of particle radius during dissolution, the mass balance expression for a dissolving spherical particle is:

$$\frac{dQ}{dt} = -4\pi a^2 \rho \frac{da}{dt} \quad (\text{eq 14})$$

where ρ is the solid density. Equation 14 is independent from eq 13. Equating eqs 13 and 14 gives:

$$4\pi a^2 DC_S \left(\frac{1}{a} + \frac{1}{h} \right) = -4\pi a^2 \rho \frac{da}{dt} \quad (\text{eq 15})$$

Rearranging eq 15 gives:

$$\frac{DC_S}{\rho h} dt = \left(-1 + \frac{h}{a+h} \right) da \quad (\text{eq 16})$$

The integral form of eq 16 is:

$$\int_0^t \frac{DC_S}{\rho h} dt = \int_{a_0}^a \left(-1 + \frac{h}{a+h} \right) da \quad (\text{eq 17})$$

Integrating both sides of eq 17 gives:

$$\frac{DC_S}{\rho h} t = a_0 - a - h \ln \frac{h+a_0}{h+a} \quad (\text{eq 18})$$

where a_0 is the initial particle radius.

Equation 18 is the general solution (in terms of particle radius) of the diffusion layer model for single spherical particle dissolution under sink conditions. The relationship between particle weight and particle radius is given by:

$$w = \frac{4}{3} \pi a^3 \rho \quad (\text{eq 19})$$

where w is particle weight and w_0 is initial particle weight.

Substituting eq 19 into eq 18 gives an expression for the change of particle weight with time:

$$\frac{DC_S}{\rho h} t = \left(\frac{3W_0}{4\pi\rho} \right)^{1/3} - \left(\frac{3W}{4\pi\rho} \right)^{1/3} - h \ln \frac{h + \left(\frac{3W_0}{4\pi\rho} \right)^{1/3}}{h + \left(\frac{3W}{4\pi\rho} \right)^{1/3}} \quad (\text{eq 20})$$

For N monodispersed particles, the total weight (W) of particles is Nw . Using this expression in eq 20 gives eq 21 which describes the dissolution process for N monodispersed particles under sink conditions with total initial weight, W_0 .

$$\frac{DC_S}{\rho h} t = \left(\frac{3W_0}{4N\pi\rho} \right)^{1/3} - \left(\frac{3W}{4N\pi\rho} \right)^{1/3} - h \ln \frac{h + \left(\frac{3W_0}{4N\pi\rho} \right)^{1/3}}{h + \left(\frac{3W}{4N\pi\rho} \right)^{1/3}} \quad (\text{eq 21})$$

Under nonsink conditions, the general dissolution equation can be derived in a similar manner (see appendix II) and is summarized below.

For N monodispersed spherical particles, the general solution in terms of particle size (a) with time is:

$$\frac{D}{\rho h V} t = \frac{1}{\beta - \alpha h^3} \{X + Y + Z\} \quad (\text{eq 22})$$

$$X = h \ln \frac{a+h}{a_0+h} - \frac{h}{3} \ln \frac{\alpha a^3 + \beta}{\alpha a_0^3 + \beta}$$

$$Y = \frac{h^2}{\gamma} \left[\frac{1}{2} \ln \frac{(\alpha a^3 + \beta)(\gamma + a_0)^3}{(\gamma + a)^3(\alpha a_0^3 + \beta)} + \sqrt{3} \tan^{-1} \left(\frac{2a - \gamma}{\sqrt{3}\gamma} \right) - \sqrt{3} \tan^{-1} \left(\frac{2a_0 - \gamma}{\sqrt{3}\gamma} \right) \right]$$

$$Z = \frac{\gamma}{3} \left[\frac{1}{2} \ln \frac{(\alpha a^3 + \beta)(\gamma + a_0)^3}{(\gamma + a)^3(\alpha a_0^3 + \beta)} - \sqrt{3} \tan^{-1} \left(\frac{2a - \gamma}{\sqrt{3}\gamma} \right) + \sqrt{3} \tan^{-1} \left(\frac{2a_0 - \gamma}{\sqrt{3}\gamma} \right) \right]$$

where α , β and γ are constants: $\alpha = 4/3\pi\rho N$, $\beta = C_S V - 4/3\pi a_0^3 \rho N$, $\gamma = (\beta/\alpha)^{1/3}$. The above general equation is not applicable when $\beta = 0$ which will lead to an indeterminate condition (i.e., division by zero). Such a situation arises when the initial particle weight (W_0) equals the amount necessary to saturate the solution (i.e., $W_0 = C_S V$). The equation for this condition is:

$$\frac{DC_S}{a_0^3 \rho N} t = \frac{1}{a} - \frac{1}{a_0} + \frac{1}{h} \ln \frac{a(a_0+h)}{a_0(a+h)} \quad (\text{eq 23})$$

Results and Discussion

1. Three Classical Particle Dissolution Rate Expressions are Special Cases of the General Solution under Sink Conditions—Two special cases of eq 18 are as follows:

(a) When $a_0 \gg h$ and $a \gg h$, eq 18 becomes (see appendix I):

$$\frac{DC_S}{\rho h} t \approx a_0 - a \quad (\text{eq 24})$$

This leads to the cube-root expression.⁵

(b) When $a_0 \ll h$, eq 18 becomes (see appendix I):

$$\frac{2DC_S}{\rho} t \approx a_0^2 - a^2 \quad (\text{eq 25})$$

This leads to the two-thirds-root expression.⁷

It is clear that both the cube-root law and the two-thirds-root expression are approximate solutions to the diffusion layer model at opposite extremes of particle size. Theoretically, the cube-root law is accurate only when the particle size is much larger than the thickness of the diffusion layer, and the two-thirds-root expression is accurate when the particle size is much smaller than the thickness of the diffusion layer.¹⁶ The square-root expression is intermediary between these two limits. It is not surprising that it fits some particle dissolution profiles, but may not describe such profiles exactly. When particle size is comparable to the thickness of the diffusion layer, the general equation provides a more accurate mathematical description.

The above conclusion can also be reached in another way. The concentration gradient at the solid-liquid interface (eq 11) can be considered to be two parts: the particle radius term (C_S/a) and diffusion layer thickness term (C_S/h). When particle size is much larger than diffusion layer thickness ($a \gg h$), the particle radius term can be omitted, we obtain $dQ/dt \approx DAC_S/h$ which will lead to the cube-root

law. On the other hand, when the particle size is much smaller than diffusion layer thickness ($a \ll h$), the diffusion layer thickness term can be omitted and we obtain $dQ/dt \approx DAC_s/a$ which leads to the two-thirds-root expression. It is obvious that both of these expressions underestimate the concentration gradient at the solid-liquid interface.

2. The Ratio between Particle Size and Diffusion Layer Thickness (a_0/h) in Controlling the Shape of a Particle Dissolution Profile—Rearranging eq 18 gives:

$$t = \frac{\rho h}{DC_s} [a_0 - a - h \ln(h + a_0) + h \ln(h + a)] \quad (\text{eq 26})$$

T can be defined as the time needed for complete dissolution (i.e., at $a = 0$) of a particle as shown below:

$$T = \frac{\rho h}{DC_s} [a_0 - h \ln(h + a_0) + h \ln(h)] \quad (\text{eq 27})$$

Dividing both sides of eq 26 by eq 27 gives:

$$\frac{t}{T} = \frac{a_0 - a - h \ln(h + a_0) + h \ln(h + a)}{a_0 - h \ln(h + a_0) + h \ln(h)} \quad (\text{eq 28})$$

Rearranging eq 28 gives:

$$\frac{t}{T} = 1 - \frac{a - h \ln(h + a) + h \ln(h)}{a_0 - h \ln(h + a_0) + h \ln(h)} \quad (\text{eq 29})$$

Further rearrangement of eq 29 gives:

$$\frac{t}{T} = 1 - \frac{a - h \ln\left(1 + \frac{a}{h}\right)}{a_0 - h \ln\left(1 + \frac{a_0}{h}\right)} \quad (\text{eq 30})$$

and

$$\frac{t}{T} = 1 - \frac{\frac{a}{a_0} - \frac{h}{a_0} \ln\left(1 + \frac{a}{a_0} \frac{a_0}{h}\right)}{1 - \frac{h}{a_0} \ln\left(1 + \frac{a_0}{h}\right)} \quad (\text{eq 31})$$

Since $a/a_0 = (w/w_0)^{1/3}$, eq 31 becomes:

$$\frac{t}{T} = 1 - \frac{\left(\frac{w}{w_0}\right)^{1/3} - \frac{h}{a_0} \ln\left[1 + \frac{a_0}{h} \left(\frac{w}{w_0}\right)^{1/3}\right]}{1 - \frac{h}{a_0} \ln\left(1 + \frac{a_0}{h}\right)} \quad (\text{eq 32})$$

Equation 32 is a dimensionless equation for single particle dissolution under sink conditions where t/T and w/w_0 can be viewed as two variables which range from 0 to 1. Plots of w/w_0 vs t/T give dissolution profiles which are independent of solid and dissolution medium used, but are governed by a_0/h . Theoretical comparisons between the general solution and classical particle dissolution expressions can be made by generating simulated particle dissolution data using eq 32 and comparing the simulated data with the traditional expressions.

If a spherical particle dissolution profile follows one of the three traditional particle dissolution expressions, one of the $(w/w_0)^{1/n}$ vs time plots ($n = 3, 2, \text{ or } 3/2$) should be linear with a slope of 1. By simulating dissolution profiles using the normalized general equation (eq 32) and plotting the resulting dissolution profiles with these three ordinate axis transformations (Figure 3), it can be seen how well

the three approximate particle dissolution rate expressions (eqs 1–3) apply. The dissolution data were simulated with different values of a_0/h . It can be seen from Figure 3 that there are deviations from linearity for some a_0/h ratios no matter what ordinate transformation is used.

It should be pointed out that linearity of such plots is not a sensitive criterion to test whether the dissolution profile is consistent with a certain rate expression. Usually dissolution profiles can be reasonably linear on any of the three transformed axes up to ~80% dissolved (i.e., $[w/w_0]^{1/n} = 0.585, 0.447, 0.342$ for $n = 3, 2, 3/2$, respectively).

3. A New Semiempirical Equation for Single Spherical Particle Dissolution under Sink Conditions—Since there are functional similarities in the three classical particle dissolution rate expressions, a new semiempirical equation (eq 33) is proposed which incorporates the three classical expressions but the exponent, n , is not limited to values 3, 2, and 3/2. The proportionality constant $k_{1/n}$ is a constant with units of mass^{1/n}/time.

$$w^{1/n} = w_0^{1/n} - k_{1/n} t \quad (\text{eq 33})$$

Single particle dissolution profiles generated from the general equation (eq 32) can be fitted by eq 33 where n ranges from 3/2 to 3 but does not have to be a specific value (i.e., 3/2, 2, or 3). If w is normalized by w_0 and t is normalized by T ($T = w_0^{1/n}/k_{1/n}$), a dimensionless expression is obtained:

$$\frac{w}{w_0} = \left(1 - \frac{t}{T}\right)^n \quad (\text{eq 34})$$

The two parameters, T and n , can be obtained by fitting eq 34 to dissolution data (w/w_0 vs t). Simulation studies were carried out at six representative a_0/h ratios. For convenience, the w/w_0 values were generated by keeping $a/a_0 = 1.0, 0.95, 0.90, \dots, 0.05, 0$ for each a_0/h ratio. The corresponding times (t) for these w/w_0 values were then calculated with eq 32. The values of T and n were obtained by fitting eq 34 to the simulated data and the results are given in Table 1. It can be seen that n depends on a_0/h with the smaller ratio giving a smaller value of n . The other fitted parameter, T , deviates slightly from its theoretical value (1.0) for all a_0/h ratios. Theoretically, it is possible to determine a_0/h from the fitted value of n . However, small variations in n can lead to dramatic changes in calculated a_0/h values making it difficult to obtain an accurate estimation of a_0/h from n .

4. Dependence of Surface-Specific Dissolution Rate upon Particle Size under Sink Conditions—According to Fick's first law,

$$J = -D \frac{\partial C}{\partial r} \quad (\text{eq 35})$$

J is the diffusional flux and is defined as the amount of substance passing per unit time normal to unit surface area. When applied to dissolution, it may also be defined as the surface-specific dissolution rate. Substituting eq 11 into eq 35 gives:

$$J = DC_s \left(\frac{1}{h} + \frac{1}{a}\right) \quad (\text{eq 36})$$

Equation 36 demonstrates that the surface-specific dissolution rate depends on particle size, with smaller particles having higher surface-specific dissolution rates (Figure 4). Bisrat et al.¹³ and Anderberg et al.^{14,17} reported a dependence of surface-specific dissolution rates upon particle size. Their results showed the same trend seen in

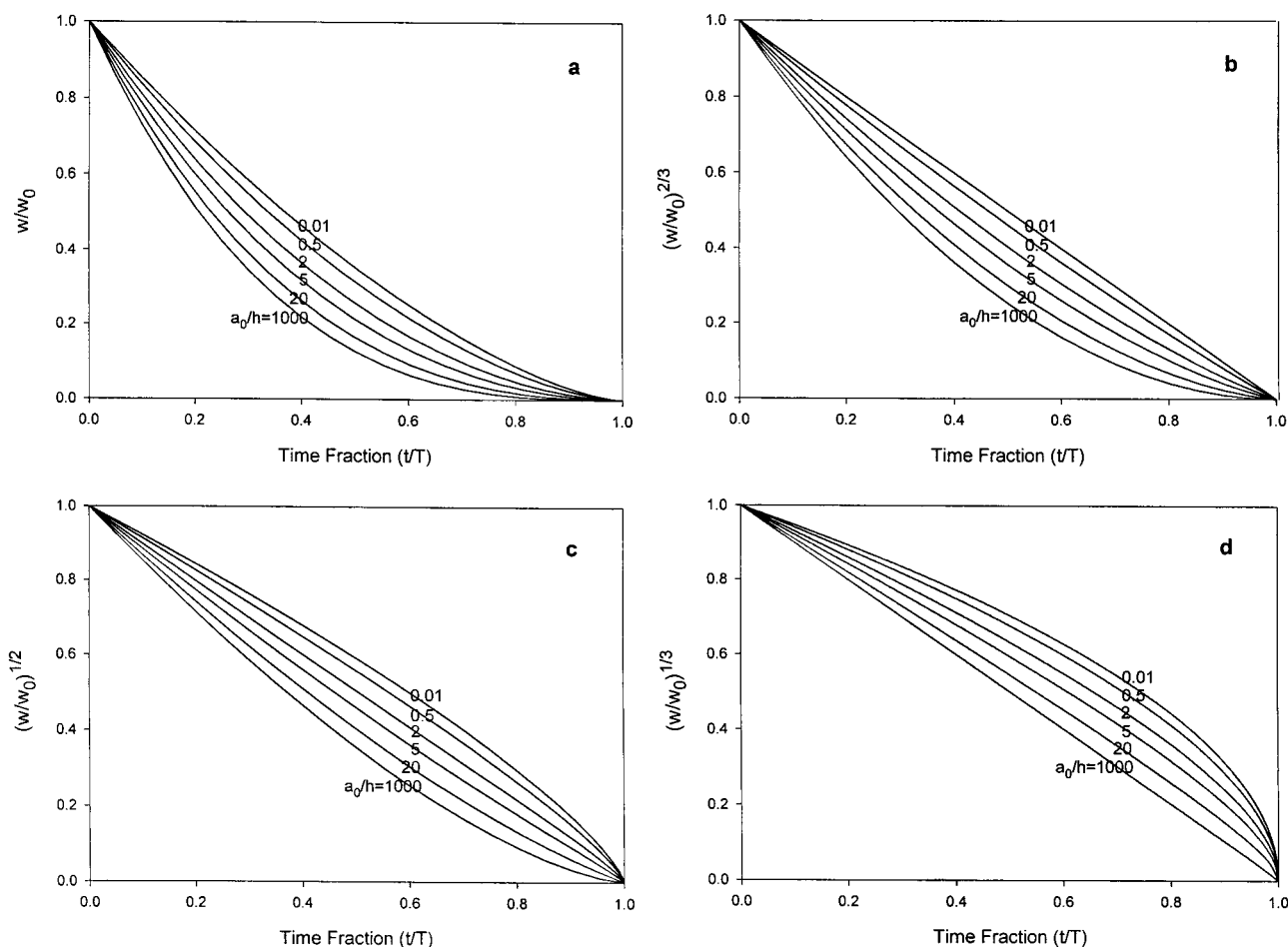


Figure 3—Simulated particle dissolution profiles (eq 32) at representative a_0/h values (0.01, 0.5, 2, 5, 20, 1000) with different $(w/w_0)^{1/n}$ ordinate axes: (a) $n = 1$; (b) $n = 3/2$; (c) $n = 2$; (d) $n = 3$.

Table 1—Fitted Parameters (n , T) for Simulated Data (eq 32) Fitted by eq 34

| a_0/h | n | T | r^2 |
|---------|------|-------|---------|
| 1000 | 3.00 | 1.004 | 1.00000 |
| 20 | 2.80 | 1.051 | 1.00000 |
| 5 | 2.43 | 1.059 | 0.99999 |
| 2 | 2.09 | 1.044 | 0.99998 |
| 0.5 | 1.71 | 1.016 | 0.99999 |
| 0.01 | 1.51 | 1.000 | 1.00000 |

Figure 4. The surface-specific dissolution rate increased (after correcting for solubility dependence on particle size) with decreasing particle size. This increase was especially pronounced for particle sizes below $\sim 5 \mu\text{m}$.

Harriott similarly reported on mass transfer to particles (i.e., particle growth) for a much wider range of particle sizes.¹⁸ He found that the mass transfer coefficient, k_c (cm/s), was almost independent of particle size for particles larger than $200 \mu\text{m}$, but was particle size dependent for smaller particles. Since diffusion layer thicknesses usually range from 10 to $200 \mu\text{m}$, it seems that for particles smaller than $200 \mu\text{m}$, particle size effects will be significant on particle dissolution.

Equation 36 can be rewritten in a more general form:

$$J = DC_s \left(\frac{1}{h} + \frac{1}{r_c} \right) \quad (\text{eq 37})$$

where r_c is the radius of curvature of a dissolving surface and is positive ($r_c > 0$) for a convex surface. For flat surfaces

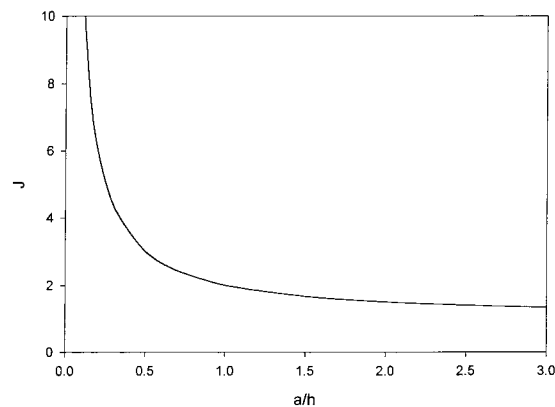


Figure 4—Relative surface-specific dissolution rate dependence (J , $J = 1$ for a flat surface) upon particle radius (a) normalized with diffusion layer thickness (h) using eq 36.

($r_c \rightarrow \infty$), dissolution rate is directly proportional to surface area. However, this simple relationship does not hold for a curved surface. Convex surfaces have larger surface-specific dissolution rates than a flat surface. Hixson and Crowell derived the cube-root law by assuming dissolution rate is proportional to particle surface area. From the above analysis we can see that this assumption is not justified when r_c is comparable to or smaller than h .

5. Particle Dissolution under Nonsink Conditions—

The general equation for spherical particle dissolution under nonsink conditions (eq 22) is algebraically complex but can be mathematically simulated. It can also be converted to particle weight (W) which will lead to an

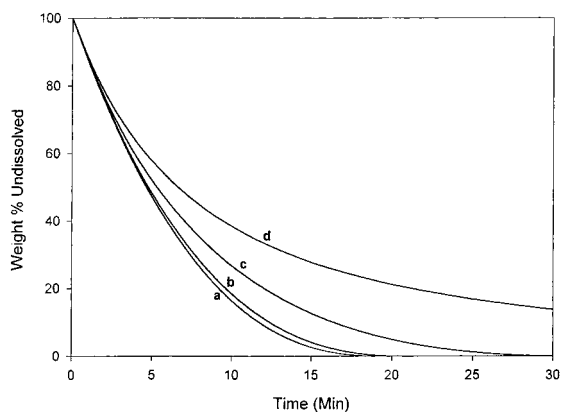


Figure 5—Comparison of particle dissolution under sink conditions (a) and three degrees of saturation: (b) 10%; (c) 50%; (d) 100%.

equally unwieldy equation which we do not show here. The main advantage of such expressions is for dissolution systems in which the drug is quite insoluble where sink conditions are difficult or impossible to maintain.

A simulation was done to compare particle dissolution under sink conditions and different degrees of nonsink conditions using eqs 21–23. Three levels of nonsink conditions were chosen: initial particle weight equal to 10%, 50%, and 100% of the amount necessary to saturate the solution. The initial particle radius was arbitrarily chosen to be 10 times as large as the diffusion layer thickness with $a_0 = 200 \mu\text{m}$, $h = 20 \mu\text{m}$, $D = 1.1 \times 10^{-5} \text{ cm}^2/\text{s}$, $C_s = 3.4 \text{ mg/mL}$, $\rho = 1.4 \text{ g/cm}^3$. A comparison of the dissolution profiles is shown in Figure 5. It can be seen that assuming sink conditions provides good results when initial particle weight is less than 10% of the weight for saturation.

Conclusions

The general solution of the diffusion layer model applied to spherical particle dissolution is derived. The three classical particle dissolution rate expressions, including the cube-root law, are special cases of the general solution to particle dissolution under sink conditions with constant diffusion layer thickness. The ratio between particle radius and diffusion layer thickness (a_0/h) is an important factor in controlling the shape of the dissolution profile. It also controls which classical model can fit a dissolution profile better than the other two models. It is necessary to apply this general equation to typical monodispersed drug powder dissolution data to fit the entire profile. This general equation will be applied to literature and experimental data in future publications.

Nomenclature

| | |
|-----------|--|
| a | particle radius |
| a_0 | initial particle radius |
| A | surface area |
| C | concentration |
| C_b | concentration in the bulk solution |
| C_s | solubility |
| D | diffusion coefficient |
| $G(R)$ | concentration gradient at distance R from the center of the particle |
| h | diffusion layer thickness |
| J | surface-specific dissolution rate, i.e., dissolution rate on unit surface area |
| $k_{1/3}$ | single particle dissolution constant in the cube-root law |

| | |
|-----------|--|
| $k_{1/2}$ | single particle dissolution constant in the square-root expression |
| $k_{2/3}$ | single particle dissolution constant in the two-thirds-root expression |
| k_n | dissolution rate constant |
| n | dissolution rate order |
| N | total number of particles |
| r | distance from the center of a particle |
| r_c | radius of curvature |
| t | time |
| T | time needed for complete particle dissolution |
| V | solution volume |
| w | individual particle weight |
| w_0 | initial individual particle weight |
| W | total weight of monodispersed particles |
| W_0 | total initial weight of monodispersed particles |
| ρ | solid density of the particle |

Appendix I

The cube-root law and the two-thirds-root expression can be derived from eq 18 using a Taylor series expansion (eq 38).

$$\ln(1+x) = x - \frac{x^2}{2} + \frac{x^3}{3} - \frac{x^4}{4} \dots \quad -1 < x \leq 1 \quad (\text{eq 38})$$

1. Derivation of the Cube-Root Law from the General Equation (eq 18). Equation 18 can be transformed to:

$$\frac{DC_s}{\rho h} t = a_0 - a + h \ln \left(1 + \frac{a - a_0}{h + a_0} \right) \quad (\text{eq 39})$$

To derive the Hixson–Crowell cube-root expression, it is necessary to assume that $h \ll a_0$ and $h \ll a$, so that $|(a - a_0)/(h + a_0)| < 1$. Applying the Taylor series expansion to eq 39 leads to:

$$\begin{aligned} \frac{DC_s}{\rho h} t &= a_0 - a + h \left[\frac{a - a_0}{a_0 + h} - \frac{1}{2} \left(\frac{a - a_0}{a_0 + h} \right)^2 + \right. \\ &\quad \left. \frac{1}{3} \left(\frac{a - a_0}{a_0 + h} \right)^3 - \frac{1}{4} \left(\frac{a - a_0}{a_0 + h} \right)^4 \dots \right] \\ &= a_0 - a + (a - a_0) h \left[\frac{1}{a_0 + h} - \frac{1}{2} \frac{(a - a_0)}{(a_0 + h)^2} + \right. \\ &\quad \left. \frac{1}{3} \frac{(a - a_0)^2}{(a_0 + h)^3} - \frac{1}{4} \frac{(a - a_0)^3}{(a_0 + h)^4} \dots \right] \\ &= (a_0 - a) \left\{ 1 - \frac{h}{a_0 + h} \left[1 - \frac{1}{2} \frac{(a - a_0)}{(a_0 + h)} + \right. \right. \\ &\quad \left. \left. \frac{1}{3} \frac{(a - a_0)^2}{(a_0 + h)^2} - \frac{1}{4} \frac{(a - a_0)^3}{(a_0 + h)^3} \dots \right] \right\} \\ &= (a_0 - a) \left\{ 1 - \frac{h}{a_0 + h} \left[1 + \frac{1}{2} \frac{a_0 - a}{a_0 + h} + \right. \right. \\ &\quad \left. \left. \frac{1}{3} \frac{(a_0 - a)^2}{(a_0 + h)^2} + \frac{1}{4} \frac{(a_0 - a)^3}{(a_0 + h)^3} \dots \right] \right\} \quad (\text{eq 40}) \end{aligned}$$

Equation 40 can be written as eq 41,

$$\frac{DC_S}{\rho h} = (a_0 - a)(1 - P) \quad (\text{eq 41})$$

For the case where $a \geq 0.5a_0$, we have $(a_0 - a)/(a_0 + h) < 1/2$, so,

$$P = \frac{h}{a_0 + h} \left[1 + \frac{1}{2} \frac{(a_0 - a)}{(a_0 + h)} + \frac{1}{3} \left(\frac{a_0 - a}{a_0 + h} \right)^2 + \frac{1}{4} \left(\frac{a_0 - a}{a_0 + h} \right)^3 \dots \right]$$

$$< \frac{h}{a_0 + h} \left[1 + \frac{1}{2} \times \frac{1}{2} + \frac{1}{3} \left(\frac{1}{2} \right)^2 + \frac{1}{4} \left(\frac{1}{2} \right)^3 \dots \right]$$

$$< \frac{h}{a_0 + h} \left[1 + \frac{1}{2} \times \frac{1}{2} + \frac{1}{2} \left(\frac{1}{2} \right)^2 + \frac{1}{2} \left(\frac{1}{2} \right)^3 \dots \right]$$

$$= \frac{3}{2} \frac{h}{a_0 + h} \quad (\text{eq 42})$$

Since $a_0 \gg h$, we have $P \ll 1$, so eq 41 can be approximated by:

$$\frac{DC_S}{\rho h} t \approx a_0 - a \quad (\text{eq 24})$$

From eq 24, the cube-root law can be derived.

2. Derivation of Two-Thirds-Root Expression from the General Equation (eq 18). Equation 18 can be transformed to:

$$\frac{DC_S}{\rho h} t = a_0 - a - h \ln \left(\frac{h + a_0}{h} \times \frac{h}{h + a} \right) =$$

$$a_0 - a - h \left[\ln \left(1 + \frac{a_0}{h} \right) - \ln \left(1 + \frac{a}{h} \right) \right] \quad (\text{eq 43})$$

In the case of the Higuchi–Hiestand two-thirds-root expression, it is necessary to assume that $h \gg a_0$ which leads to $a_0/h \ll 1$. Applying the Taylor series expansion to eq 43 gives:

$$\frac{DC_S}{\rho h} t = a_0 - a - h \left[\frac{a_0}{h} - \frac{1}{2} \left(\frac{a_0}{h} \right)^2 + \frac{1}{3} \left(\frac{a_0}{h} \right)^3 \dots - \frac{a}{h} + \frac{1}{2} \left(\frac{a}{h} \right)^2 - \frac{1}{3} \left(\frac{a}{h} \right)^3 \dots \right] \quad (\text{eq 44})$$

Since $a_0/h \ll 1$, eq 44 can be approximated by:

$$\frac{DC_S}{\rho h} t \approx a_0 - a - h \left[\frac{a_0}{h} - \frac{1}{2} \left(\frac{a_0}{h} \right)^2 - \frac{a}{h} + \frac{1}{2} \left(\frac{a}{h} \right)^2 \right] =$$

$$\frac{1}{2} \frac{(a_0^2 - a^2)}{h} \quad (\text{eq 45})$$

Rearranging eq 45 gives:

$$\frac{2DC_S}{\rho} t \approx a_0^2 - a^2 \quad (\text{eq 25})$$

From eq 25 the two-thirds-root expression of Higuchi and Hiestand can be derived.

Appendix II

The general solution for single spherical particle dissolution under nonsink conditions can also be derived in a

similar manner as under sink conditions. If the initial bulk concentration is 0 and the solution volume (V) is kept constant, the bulk concentration (C_b) can be described by the following equation for single spherical particle dissolution:

$$C_b = \frac{\frac{4}{3}\pi(a_0^3 - a^3)\rho}{V} \quad (\text{eq 46})$$

Under nonsink conditions, eqs 5–8 are still valid, while eq 10 should be modified to give:

$$\int_a^{a+h} -\frac{a^2}{r^2} G(a) dr = C_S - C_b \quad (\text{eq 47})$$

Integrating eq 47 gives:

$$G(a) = -\left(\frac{1}{a} + \frac{1}{h} \right) (C_S - C_b) \quad (\text{eq 48})$$

Substituting eq 48 into eq 6 gives:

$$\frac{dQ}{dt} = 4\pi a^2 D \left(\frac{1}{a} + \frac{1}{h} \right) (C_S - C_b) \quad (\text{eq 49})$$

Equating eq 14 and eq 49 and rearranging gives:

$$-\frac{D}{\rho h} dt = \frac{a}{(a+h)(C_S - C_b)} da \quad (\text{eq 50})$$

The integral form of eq 50 is:

$$\int_0^t -\frac{D}{\rho h} dt = \int_{a_0}^a \frac{a}{(a+h)(C_S - C_b)} da \quad (\text{eq 51})$$

Substituting eq 46 into eq 51 gives:

$$\int_0^t -\frac{D}{\rho h} dt = \int_{a_0}^a \frac{a}{(a+h) \left(C_S - \frac{4}{3V}\pi a_0^3 \rho + \frac{4}{3V}\pi a^3 \rho \right)} da \quad (\text{eq 52})$$

Integrating eq 52 will lead to a relationship between particle radius and time. The integration is complex and only the final form is given below:

$$\frac{D}{\rho h V} t = \frac{1}{\beta - \alpha h^3} \{ X + Y + Z \} \quad (\text{eq 22})$$

$$X = h \ln \frac{a+h}{a_0+h} - \frac{h}{3} \ln \frac{\alpha a^3 + \beta}{\alpha a_0^3 + \beta}$$

$$Y = \frac{h^2}{\gamma} \left[\frac{1}{2} \ln \frac{(\alpha a^3 + \beta)(\gamma + a_0^3)}{(\gamma + a)^3(\alpha a_0^3 + \beta)} + \right.$$

$$\left. \sqrt{3} \tan^{-1} \left(\frac{2a - \gamma}{\sqrt{3}\gamma} \right) - \sqrt{3} \tan^{-1} \left(\frac{2a_0 - \gamma}{\sqrt{3}\gamma} \right) \right]$$

$$Z = \frac{\gamma}{3} \left[\frac{1}{2} \ln \frac{(\alpha a^3 + \beta)(\gamma + a_0^3)}{(\gamma + a)^3(\alpha a_0^3 + \beta)} - \right.$$

$$\left. \sqrt{3} \tan^{-1} \left(\frac{2a - \gamma}{\sqrt{3}\gamma} \right) + \sqrt{3} \tan^{-1} \left(\frac{2a_0 - \gamma}{\sqrt{3}\gamma} \right) \right]$$

In eq 22, α , β and γ are constants: $\alpha = 4\pi\rho/3$, $\beta = C_S V - 4\pi a_0^3 \rho/3$, $\gamma = (\beta/\alpha)^{1/3}$. For N monodispersed particles, eq

22 is essentially the same except that $C_b = [4\pi(a_0^3 - a^3)\rho N/3]/V$, correspondingly, the values of α and β become $\alpha = 4/3\pi\rho N$, $\beta = C_S V - 4/3\pi a_0^3\rho N$. Weight undissolved (w) expressions can be obtained by substituting $a = (3w/4\pi\rho)^{1/3}$ in eq 22.

A special case arises when the initial particle weight (w_0) exactly equals the amount necessary to saturate the solution. In this case, the above equation does not work ($\beta = 0$) and a special equation needs to be derived where:

$$C_S = \frac{4}{3V}\pi a_0^3\rho \quad (\text{eq 53})$$

Thus, eq 52 becomes:

$$\int_0^t -\frac{D}{\rho h} dt = \int_{a_0}^a \frac{1}{\frac{4}{3V}\pi a^2\rho(a+h)} da \quad (\text{eq 54})$$

Integrating both sides of eq 54 gives:

$$\frac{4D\pi}{3V} t = \frac{1}{a} - \frac{1}{a_0} + \frac{1}{h} \ln \frac{a(a_0+h)}{a_0(a+h)} \quad (\text{eq 55})$$

Substituting for V using eq 53 into the left-hand side of eq 55 gives:

$$\frac{DC_S}{a_0^3\rho} t = \frac{1}{a} - \frac{1}{a_0} + \frac{1}{h} \ln \frac{a(a_0+h)}{a_0(a+h)} \quad (\text{eq 56})$$

For N monodispersed particles, $C_S = 4\pi a_0^3\rho N/3V$ and the final equation becomes:

$$\frac{DC_S}{a_0^3\rho N} t = \frac{1}{a} - \frac{1}{a_0} + \frac{1}{h} \ln \frac{a(a_0+h)}{a_0(a+h)} \quad (\text{eq 23})$$

References and Notes

- Noyes, A.; Whitney, W. R. The Rate of Solution of Solid Substances in their own Solutions. *J. Am. Chem. Soc.* **1897**, *19*, 930–934.
- Nernst, W. Theorie der Reaktionsgeschwindigkeit in Heterogenen Systemen. *Z. Physik. Chem.* **1904**, *47*, 52–55.
- Brunner, E. Reaktionsgeschwindigkeit in Heterogenen Systemen. *Z. Physik. Chem.* **1904**, *47*, 56–102.
- King, C. V. Reaction Rates at Solid–Liquid Interfaces. *J. Am. Chem. Soc.* **1935**, *57*, 828–831.
- Hixson, A. W.; Crowell, J. H. Dependence of Reaction Velocity upon Surface and Agitation I – Theoretical Consideration. *Ind. Eng. Chem.* **1931**, *23*, 923–931.
- Niebergall, P. J.; Milosovich, G.; Goyan, J. E. Dissolution Rate Studies II. Dissolution of Particles Under Conditions of Rapid Agitation. *J. Pharm. Sci.* **1963**, *52*, 236–241.
- Higuchi, W. I.; Hiestand, E. N. Dissolution Rates of Finely Divided Drug Powders I. Effect of a Distribution of Particle Size in a Diffusion-Controlled Process. *J. Pharm. Sci.* **1963**, *52*, 67–71.
- Hixson, A. W.; Crowell, J. H. Dependence of Reaction Velocity upon Surface and Agitation II – Experimental Procedure in Study of Surface. *Ind. Eng. Chem.* **1931**, *23*, 1002–1009.
- Higuchi, W. I.; Rowe, E. L.; Hiestand, E. N. Dissolution Rates of Finely Divided Drug Powders II. Micronized Methylprednisolone. *J. Pharm. Sci.* **1963**, *52*, 163–164.
- De Almeida, L. P.; Simões, S.; Brito, P.; et al. Modeling Dissolution of Sparingly Soluble Multisized Powders. *J. Pharm. Sci.* **1997**, *86*, 726–732.
- Pedersen, V. P.; Brown, K. F. Experimental Evaluations of Three Single-Particle Dissolution Models. *J. Pharm. Sci.* **1976**, *65*, 1442–1447.
- Lu, A. T. K.; Frisella, M. E.; Johnson, K. C. Dissolution Modeling: Factors Affecting the Dissolution Rates of Polydisperse Powders. *Pharm. Res.* **1993**, *10*, 1308–1314.
- Bisrat, M.; Nyström, C. Physicochemical Aspects of Drug Release. VIII. The Relation between Particle Size and Surface-Specific Dissolution Rate in Agitated Suspensions. *Int. J. Pharm.* **1988**, *47*, 223–231.
- Anderberg, E. K.; Nyström, C. Physicochemical Aspects of Drug Release X. Investigation of the Applicability of the Cube-Root Law for Characterization of the Dissolution Rate of Fine Particulate Materials. *Int. J. Pharm.* **1990**, *62*, 143–151.
- Steady-state and pseudo-steady-state are important concepts in this paper. Dissolution from a planar surface under sink conditions reaches steady-state when the dissolution rate becomes constant; hence, the concentration gradient in the diffusion layer becomes time-invariant. Dissolution of a spherical surface will not reach steady-state because its surface area decreases with time and the concentration gradient is not time-invariant. However, a pseudo-steady-state may exist in which the following approximation is accurate—the overall mass transport rates across the inner and outer spherical surfaces (at $r = a$ and $a + h$) of the diffusion layer are equal. This assumption requires that within the time for an average molecule to cross the diffusion layer, the change of particle surface area is negligible.
- In the derivation of the two-thirds-root expression (Higuchi and Hiestand), it was assumed that the fluid is perfectly stagnant and the diffusion equation for spherical geometry was solved. This case is mathematically equivalent to assuming a linear concentration gradient in a diffusion layer of thickness equal to the particle radius. This mathematical identity is just a coincidence and does not have any mechanistic significance.
- Anderberg, E. K.; Bisrat, M.; Nyström, C. Physicochemical Aspects of Drug Release VII. The Effect of Surfactant Concentration and Drug Particle Size on Solubility and Dissolution Rate of Felodipine, a Sparingly Soluble Drug. *Int. J. Pharm.* **1988**, *47*, 67–77.
- Harriott, P. Mass Transfer to Particles: Part I. Suspended in Agitated Tanks. *AIChE J.* **1962**, *8*, 93–101.

JS980236P